

Beam-based measurements of long-range transverse wakefields in the Compact Linear Collider main-linac accelerating structure

Hao Zha,¹ Andrea Latina,¹ Alexej Grudiev,¹ Giovanni De Michele,^{1,2,3} Anastasiya Solodko,¹ Walter Wuensch,¹ Daniel Schulte,¹ Erik Adli,^{4,5} Nate Lipkowitz,⁴ and Gerald S. Yocky⁴

¹CERN, European Organization for Nuclear Research, 1211 Geneva, Switzerland

²PSI, Paul Scherrer Institut, 5232 Villigen, Switzerland

³EPFL, École Polytechnique Fédérale de Lausanne, 1015 Lausanne, Switzerland

⁴SLAC National Laboratory, 2575 Sand Hill Road, Menlo Park, California 94025, USA

⁵Department of Physics, University of Oslo, 0316 Oslo, Norway

(Received 15 May 2015; published 20 January 2016)

The baseline design of CLIC (Compact Linear Collider) uses X-band accelerating structures for its main linacs. In order to maintain beam stability in multibunch operation, long-range transverse wakefields must be suppressed by 2 orders of magnitude between successive bunches, which are separated in time by 0.5 ns. Such strong wakefield suppression is achieved by equipping every accelerating structure cell with four damping waveguides terminated with individual rf loads. A beam-based experiment to directly measure the effectiveness of this long-range transverse wakefield and benchmark simulations was made in the FACET test facility at SLAC using a prototype CLIC accelerating structure. The experiment showed good agreement with the simulations and a strong suppression of the wakefields with an unprecedented minimum resolution of 0.1 V/(pC mm).

DOI: 10.1103/PhysRevAccelBeams.19.011001

I. INTRODUCTION

The main linac of the Compact Linear Collider (CLIC) uses X-band normal conducting accelerating structures. The motivation for this technology choice is to achieve a higher accelerating gradient and a shorter accelerator length, which extends the energy reach and is potentially cheaper. CLIC rf frequency is 12 GHz and the gradient is 100 MV/m [1]. One of the main challenges to emerge from the choice of such a high frequency is the strong long-range wakefields.

In order to increase luminosity while minimizing the power consumption, multiple-bunch trains are accelerated in each rf pulse which increases the efficiency of the transfer of rf power to the beam. The CLIC baseline beam is a train of 312 bunches with an intratrain bunch-to-bunch distance of 0.5 ns, or 15 cm at the speed of light. When many bunches are accelerated in a train one of the most important limitation to the luminosity is given by the emittance growth due to bunch-to-bunch instabilities caused by coupling through transverse wakefields. In particular transverse misalignments between the beam and the rf structures result in the excitation of long-range transverse wakefields, which kick the following bunches. Dedicated beam dynamics studies indicate that the

transverse wakefield kick of a bunch on the following bunch must be suppressed to less than 6.6 V/(pC m mm), in order to maintain the beam stability in the main linac [2]. Reference [2] reports that randomly jittering bunches experience a factor 4 increase in the projected emittance growth with the wakefield kick at this limiting value. This is the maximum consistent with the emittance growth budget in the CLIC design.

The current CLIC baseline main linac accelerating structure is referred to as CLIC-G design [3]. The CLIC-G design uses both waveguide damping (see Fig. 1) and cell-to-cell detuning to provide strong broadband suppression of the long-range wakefields. The waveguides are dimensioned so that the cutoff frequency is above the operating frequency in order to prevent degradation of fundamental mode Q . The cell geometry and rf loads have been extensively optimized in order to maximize efficiency, high-gradient, rf performance, and to meet the beam

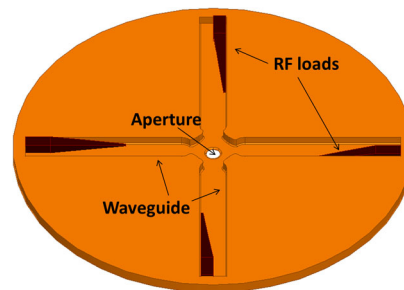


FIG. 1. Geometry of single CLIC-G cell.

Published by the American Physical Society under the terms of the Creative Commons Attribution 3.0 License. Further distribution of this work must maintain attribution to the author(s) and the published article's title, journal citation, and DOI.

dynamics constraints. Details of the design and the design process are described in [3]. High-power tests of CLIC-G prototypes are now underway and consistently show gradients in the range of 100 MV/m [4,5].

Due to the importance of the long-range transverse wakefield suppression, an experimental verification of this aspect of the CLIC-G design has been given high priority. The aim of this demonstration is twofold: validate that the beam dynamics requirements are met, and prove that the computer-simulated transverse wakefields are accurate. This latter condition is essential since the design may evolve in the future. The experimental demands are significant since the suppression must be measured at bunch distances from the peak of the transverse wakefield to the end of CLIC bunch train, which is spanning more than 4 orders of magnitude, namely from 1 mm to 50 m and over approximately 3 orders of magnitude of wakefield level. These very stringent measurement requirements can currently be met only at the FACET facility [6] in the SLAC National Accelerator Laboratory. The particular feature of this facility, which is so important for this type of measurement, is that it can simultaneously deliver positron and electron bunches. This gave us the possibility of exciting wakes with a positron bunch and then measuring the transverse kick directly on a following electron bunch at variable distance.

A schematic of the measurement scheme is shown in Fig. 2. The positron beam (*driver* bunch) passes through the structure under test with a tunable transverse offset, thus generating a transverse wakefield. The following electron bunch (*witness* bunch) is then deflected by this wakefield. Downstream of the structure, a dipole magnet splits the trajectories of the driver and witness bunches. The positron bunch is dumped, and the deflection of the electron orbit is measured by the following beam positron monitors (BPMs). The wakefield is then deduced from the perturbation of the electron orbit.

A first direct wakefield measurement was previously made at AATF (Argonne Advanced Accelerator Test Facility) using two electron beams (at energy 5/20 MeV), to test the wakefield of next linear collider project (NLC) structures [7]. For the NLC structures a similar measurement was performed at the ASSET facility, using GeV electron and

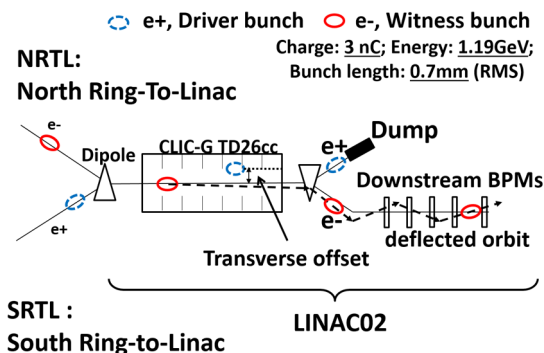


FIG. 2. Layout of the experiment.

positron beams to gain higher precision [8]. Wakefield measurements of C-band choke-mode structure [9], as well as the 30 GHz CLIC accelerating structure [10], were also performed at the ASSET facility. The measurement presented in this report represents a significant step forward in better resolution compared to any previous experiment. This was achieved by using advanced linac alignment and trajectory correction algorithms [11], as it will be described in subsequent sections.

Indirect wakefield measurements using only a single electron bunch have also been performed for wakefield-transformer structures [12], choke-mode cavities [9], and photonic-band-gap structures [13,14]. In these kinds of measurements the wakefield signal is picked up by an rf probe in the structure. It is an indirect measurement that does not allow full wakefield reconstruction, for example of trapped modes.

II. EXPERIMENT SETUP

A dedicated test structure was built to carry out the measurement here reported. A 3D model of the test structure is shown in Fig. 3. The geometry was the same as the so-called CLIC-G, that is the 3 TeV baseline accelerating structure design [3]. The structure was composed of aluminium disks clamped together with bolts. This simplified construction was acceptable since the loaded Q of the dipole mode is very low, of the order of 10, and the test structure would not see high powers. The damping waveguides were terminated by silicon carbide rf loads, assembled in groups in a comblike structure.

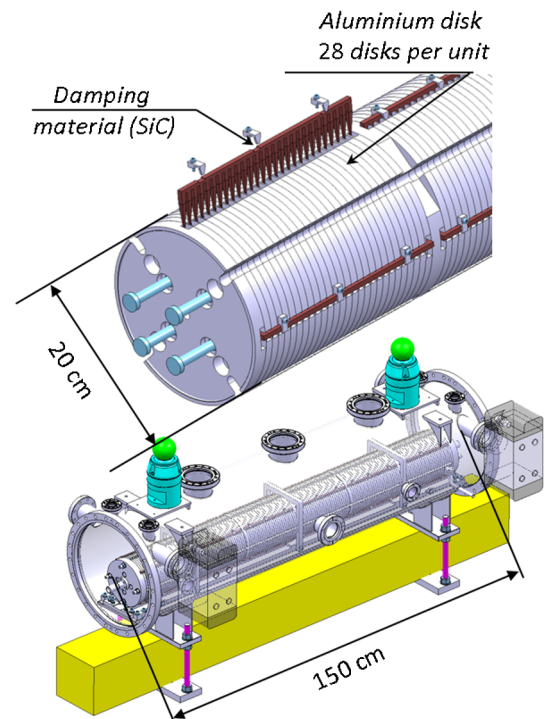


FIG. 3. The tested CLIC-G prototype structure.

The total length of the test structure was 1.6 m, which corresponds to six identical structure units. The total length was chosen so that the structures would give an integrated wakefield strong enough to be resolved in the FACET facility, even after 2 orders of magnitude suppression expected. The target resolution of this experiment was set to be less than 1 V/(pC mm). At this level of wakefield, a 3 nC positron bunch with 1.2 mm transverse offset will generate 5 keV transverse kick to the following electron bunch in the test structure.

In the measurement, the positron bunch was deflected so that it traveled through the structure with a tunable transverse offset in order to induce a dipolar transverse wakefield. The offset of the positron bunch was controlled using orbit bumps excited using upstream correctors. The strength of the correctors needed to give a desired transverse offset was calculated from the trajectory response matrix, that is the response of the BPM readings to the strength of each upstream corrector. The trajectory response matrix was measured with great accuracy using the tools developed for the beam-based alignment experiment described in [15].

In order to measure the long-range transverse wakefield with a fine time resolution, and to reconstruct the wakefield spectrum up to 50 GHz, a control and knowledge of the longitudinal spacing between the electron and positron bunches at the level of 3 mm is needed. In the FACET facility, this was possible by changing the positrons “kick-out” rf bucket and the synchronized rf phase in the south ring to linac line, to control the relative spacing while the timing of the electron bunches is left unchanged. The kick-out rf bucket determines the timing of the positron delivery into the linac in steps of S-band periods, i.e., 350 ps, providing the coarse timing control. A finer, continuous, timing control within an S-band period was achieved by varying the synchronous phase. Such a fine rf phase control system has been proved to be very stable pulse-to-pulse at the subpicosecond level [8].

The transverse wakefield was calculated from the measured offsets of the electron bunch in the downstream BPMs according to Eq. (1). In the formula Q_p is the positron charge (3 nC), E_e is the kinetic energy of the electron bunch in the structure (1.19 GeV); and L is the total active length of the structure under test (1.38 m). Δy_p is the transverse offset of the driving positron bunch and Δy_e is the measured deflection of the electron beam in the downstream BPMs. R_{12}^- is the response matrix of the BPMs to a transverse kick:

$$\Delta y_e = \Delta y_p \frac{R_{12}^-}{E_e} Q_p L W_{\perp}(s). \quad (1)$$

W_{\perp} is the unknown wakefield expressed in units of length. The absolute value of transverse wakefield relies on knowing all variables in Eq. (1) before measuring the

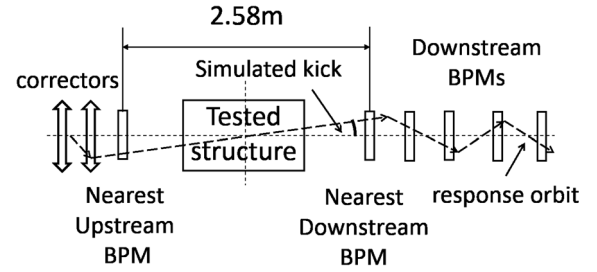


FIG. 4. R_{12}^- (response orbit) measurements by simulating the wake kick using upstream correctors.

wakefield. The term R_{12}^- represents the response of the downstream electron BPMs to a kick located in the middle of the structure. However, since there were no correctors in the center of the structure, R_{12}^- was not directly measurable. We computed the response by interpolation, sampling the orbit response to the upstream correctors (see Fig. 4) and inferring the response to a hypothetical kicker located in the center of the structure from the downstream BPMs. The nearest upstream and downstream BPMs were used to monitor the virtual kick. Two quadrupoles were located very close to the BPMs (5 cm), however this distance is far smaller than the distance between two BPMs, which is 3 m, and the effect of quadrupoles could be neglected. In the downstream beam line, 26 BPMs were used to measure the deflected electron bunch orbit. Thus, R_{12}^- of all 26 downstream BPMs (so-called the response orbit) were measured. The slope of linear fit on BPM readings and corresponding R_{12}^- gives the value of kick referenced to the center of the structure.

Dispersion free steering (DFS) was applied to the entire beam line in order to reduce the effects of energy jitter on the electron bunch orbit through residual dispersion. The dispersion correction was performed using the technique described in [11] i.e., by adjusting the strength of the correctors to cancel any dispersive effects due to misaligned magnets. In this technique the dispersion is typically measured by observing the orbit change due to a beam energy change. The energy change is usually performed by changing the phase of some klystrons. The simultaneous presence of positrons and electrons in the upstream part of LINAC02 allowed one to measure the dispersion with even higher accuracy: since a positron beam is deflected by a magnetic field oppositely to an electron beam, the motion of a positron beam is equivalent to the motion of an electron beam with negative energy, which effectively gives a very large dispersion. A measure of the dispersion after correction showed that the dispersion in the downstream part of LINAC02 was reduced by 2/3 after DFS.

The preliminary calibration of the orbits completed, the measurement of the long range transverse wakefield could be performed. The vertical transverse wakefield was sampled at 252 different bunch distances. For each spacing several transverse offsets of positron were used, ranging

from -1.2 mm to $+1.2$ mm in steps of 0.4 or 0.6 mm. The electron orbit was measured and averaged over 100 pulses, in order to reduce the noise due to fast jitters and gain in resolution. Since the positron bunch charge could not be measured when the electron bunch was present, the electron bunch was switched off periodically to check the positron charge. This measurement, in agreement with a FACET monitor displaying the charge profile, showed that the positron charge jitter is less than 2% ; this was within the acceptable level for our kick reconstruction. Preliminary analyses of the results were presented at [16].

III. RESULTS AND DISCUSSION

The transverse wakefield was calculated from the measured trajectories of electron bunches based on Eq. (1). A reference trajectory was recorded in the case the positron was absent. Δy_e were the difference of the deflected trajectory to the reference one. The wakefield kick k of one trajectory is calculated by linear fit of Δy_e of all BPM readings to the response orbit R_{12}^- .

Trajectories of electron bunches were measured with different transverse offsets Δy_p of the positron bunches. The deflection k of each trajectory is a linear function of Δy_p , of which the slope is the dipolar transverse wakefield value (see Fig. 5). The misalignment of the test structures and the beam line (within $100 \mu\text{m}$) will only change the intercept of this linear function and will not affect the dipolar transverse wakefield results directly.

Figure 6 shows plots of measured time-dependent transverse wakefield results on two different time scales. The measured wakefields are also compared with GDFIDL [17] simulations of the same geometry, using positron and electron bunch lengths equal to experimental ones. Details of the simulation are introduced in Appendix B.

The resolution of the measured wakefield was calculated from the deviation of repeatedly measured data sets (details are introduced in Appendix A). The minimum resolution

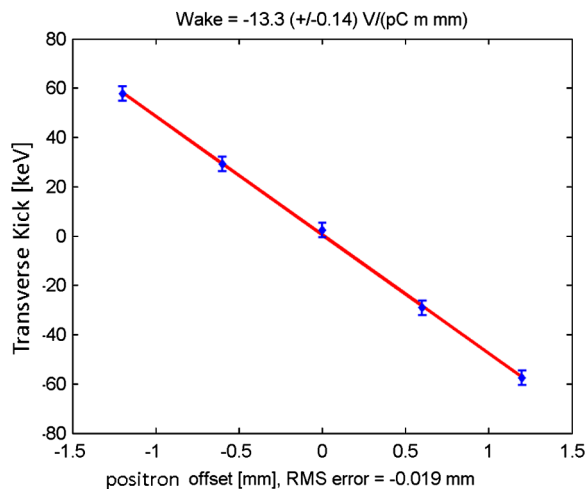


FIG. 5. Calculation of transverse wakefield.

achieved in the measurements was 0.1 V/(pC m mm). This resolution value was about 1% – 2% of the wakefield amplitude, which means that the error bars are barely visible in the plots (yet they are displayed). By observing plots in e.g., [8,9], it seems that the resolution in such experiments was about 10% of the measured wakefield value, 1 order of magnitude less accurate than the measurement presented in this paper. Better agreement between measured data and simulated ones is also appreciable in this measurement.

At the CLIC bunch spacing of 15 cm, the measured transverse wakefield kick is 5 V/(pC m mm) and meets the requirement determined by beam dynamics. The wakefield continues to fall rapidly and at larger numbers of bunch separations the wakefield potential drops to the range of 0.01 – 0.1 V/(pC m mm), which corresponds to the resolution limit of the measurement.

The minimum resolution obtained in the original measured data without any further correction was 0.5 V/(pC m mm). One of the main error sources comes from the electron orbit drift, which was observed in both cases where the positron beam was present and not present. Singular value decomposition (SVD) is the usual method to discover certain patterns from repeatedly measured orbit

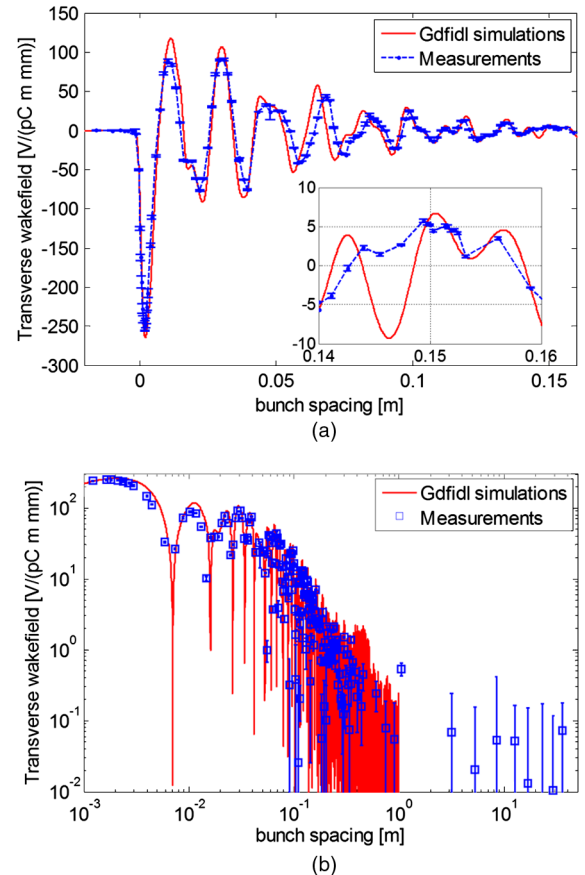


FIG. 6. Measured time-dependent wakefield: (a) partial data (linear scale); (b) full data (log scale).

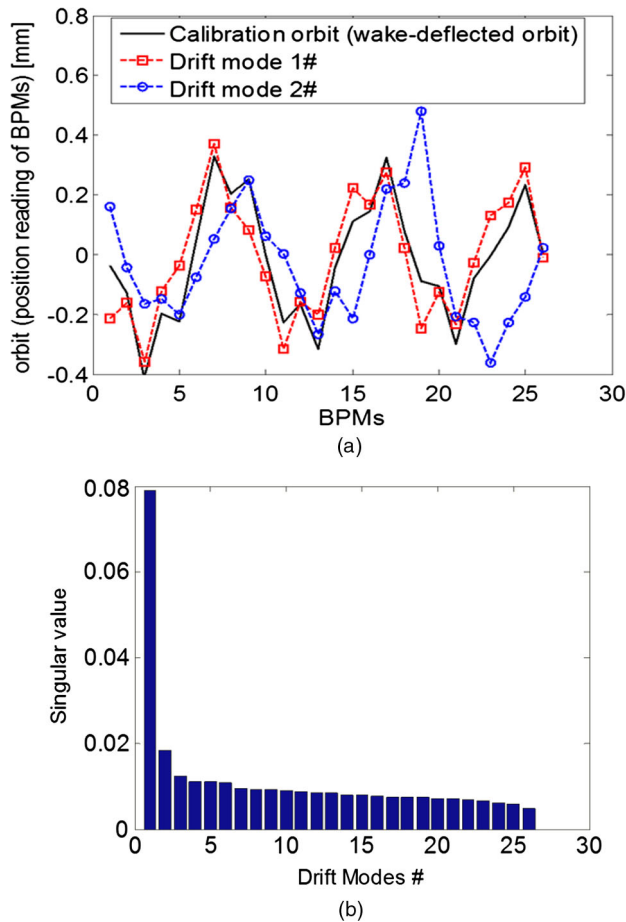


FIG. 7. (a) Patterns of wake-deflected orbit and drift orbits. (b) SVD Eigenvalue (strength) of all drift modes.

[18]. We collected all measured electron orbits in the case that the positron was not present, meaning no wakefield kick and only orbit drift. By using SVD to decompose those orbits, the drift was dominated by a few patterns (modes) as shown in Fig. 7. The first-order pattern was similar to a betatron-like oscillation but in a different phase to the wakefield kick. We suspected it was due to ripple current of upstream kickers. The second-order pattern was similar to a dispersive drift. Probably because the DFS alignment algorithm was used, this drift mode was much smaller than the first-order one.

Figure 8 shows a drift-free correction can be applied to the measured results. Each orbit can be expressed as a vector in N -dimension Euclidean space, where N is the number of BPMs. The calculated wakefield value would be the slope of a linear fit to the measured orbits on the response orbit. This is equivalent to the inner product of two vectors in N -dimension space. The real measured orbits are a linear combination of wakefield kicked modes and drift modes. The amplitude of drift mode component in the measured orbits is not necessarily stable from pulse to pulse. As seen in Fig. 7(a), the profiles of drift modes were already precalculated from all measured electron orbits

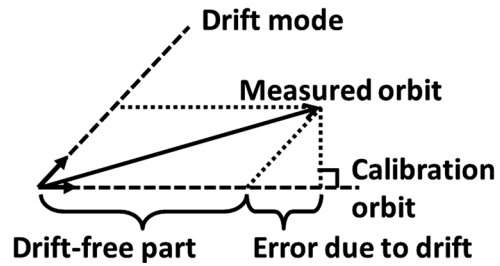


FIG. 8. Drift-mode removal of measured orbit.

without any wakefield kick. The angle between the first/second major drift mode and the response orbit in the N -dimension space is $39/53$ degree. The drift modes and the response orbit were not orthogonal to each other, meaning that there will be projection from the drift modes on the wakefield kicked one as seen in Fig. 8. This projection increased the pulse-to-pulse uncertainty to the results. Nonorthogonal vector decomposition (parallelogram rule extended to N -dimension) could be used to remove the interference from the drift orbit modes. The drift correction improved the resolution on the points having weak wakefield signal to $0.1\text{--}0.15$ V/(pC m mm). However, due to the error of measuring response orbit, this drift correction introduces another error proportional to the signal strength. Thus for those spacings having a strong wakefield, the drift correction may increase the error and it is better to not do the drift-free correction. Consequently each point was calculated in both ways and the one with lower error was selected.

An apparent timing error, that is an error in the spacing between positron and electron bunches, can be seen when comparing measured data with simulation results [see Fig. 6(a)]. In addition a significant, 300 MHz, frequency difference between measurement and simulation for the first dipole band can be seen. Also nonphysical peaks, those in which the frequency is not harmonically related to the dipole modes in this test structure, appeared in the spectrum.

According to SLAC linac experts, the calibration error of the electronic phase shifter in the rf phase control system is believed to be about 2% of an rf period. Since this error acts differently on the electron and positron bunches, this could explain the time difference observed in Fig. 6. However, the calibration error was not directly measurable in the FACET facility when the measurement was done and can only be analyzed off-line. This can be done by first assuming it is a real effect and attempting to artificially correct the timing disagreement. The timing shifts between measurement and simulation shown in Fig. 9(a) are calculated by comparing the longitudinal position of each peak or valley for the wakefield value in the measured and simulated data. The shifts appear to be a periodic function of the synchronous rf phase. This is consistent with the believed calibration error in the rf phase shifter, so a sine function was then used for timing correction. Following the timing correction

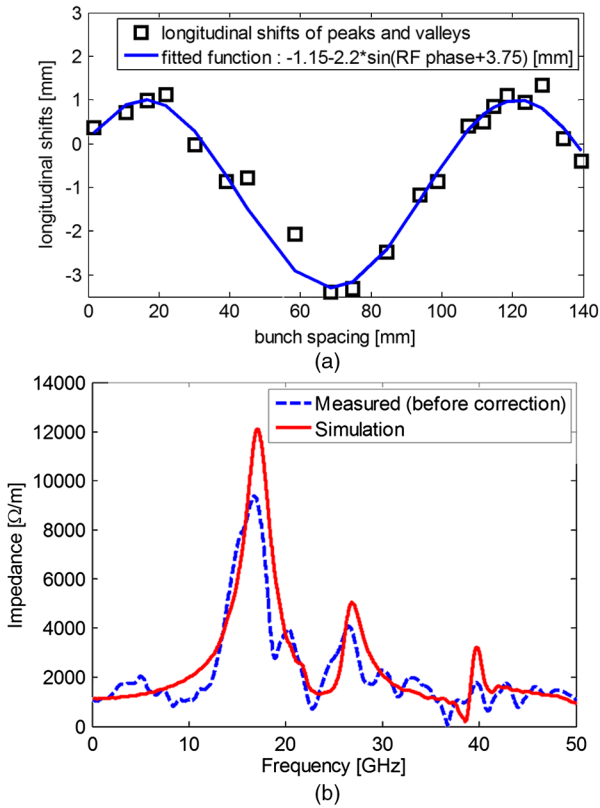


FIG. 9. (a) Timing shift of measured data to the simulated one. (b) Spectrum of original measured data.

[see Fig. 10(a)], the measured wakefield shows less timing disagreement to the simulated data. The spectrum of the measured one after the timing correction is plotted in Fig. 10(b), which is in excellent agreement with the simulated one in frequency and the nonphysical peaks disappear. This means that it is likely that the timing shift was a real effect and that it is reasonable to apply the timing correction to the measured data.

By looking closely an additional discrepancy between the simulated and measured wakefield appears. As seen in Fig. 6(a) the measured wakefield value was lower than the simulated one. The averaged amplitude difference between them is about 10%. Possible explanations related to the measuring are listed below.

(1) The response orbit was measured repeatedly by the tools [15] to get a converged data set (change less than 1%). We managed to get three data sets of response orbit in different days, and the difference among them was less than 0.8%. On the other hand, the profile of response orbit is very similar to the measured wake-deflected orbit (with correlation coefficient is 0.9997), which proved that the response orbit measuring was accurate compared to the 10% difference.

(2) The positron orbit bumping was checked before and after every time shift, and disagreements between the measured positron transverse offset and the target one was less than 2%.

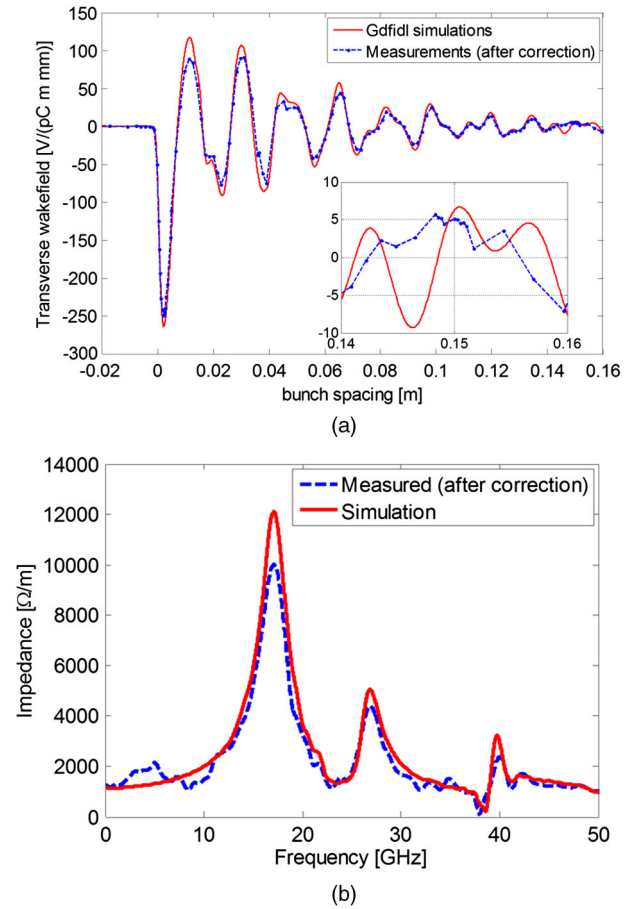


FIG. 10. (a) Wakefield plots after artificially correction on the timing shift. (b) Spectrum of measured data after timing correction.

(3) The positron charge, which contributes linearly to the wakefield amplitude, was stable during the whole experiment (overall change was less than 2%).

(4) The measured bunch length was 700 μm for both electron and positron beams. Different bunch length will change the wakefield amplitude and especially the wakefield profile near the overlapping of electrons and positrons. In Fig. 11 we proposed using the rise time to examine the

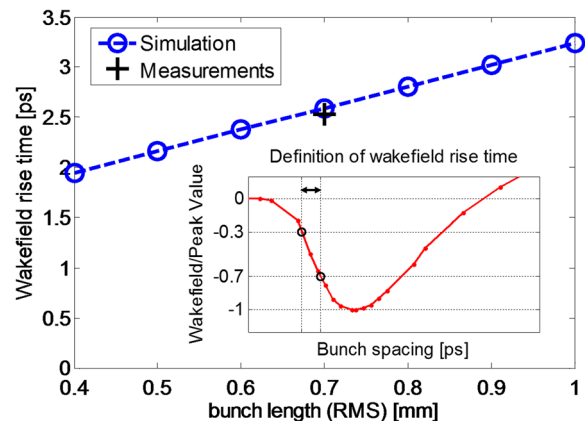


FIG. 11. Rise time of measured and simulated wakefield.

effect of the bunch length. The rise time here is defined as the time interval of the wakefield to rise from 30% to 70% of its peak value, since there were too few measured data below 30% of the peak value. As shown in Fig. 11, the rise time of measured wakefield is very close to the simulated one using 700 μm bunch length, and changing the bunch length by 100 μm only changes 2% of the amplitude. Thus the bunch length is not likely the reason.

Therefore, these four issues related to the measuring were not likely the reason of the 10% difference. The discrepancy can also possibly come from the simulation, e.g., material of rf load, meshing of geometry, numeric error, etc. The rf load can only affect the wakefield with bunch spacing more than 10 cm (distance from beam axis to the rf load is 5 cm) and is not likely the reason of the 10% difference. As introduced in Appendix B, Simulation on different meshing size was also carried out and no significant difference on the initial amplitude was observed.

In conclusion, the 10% difference between the measured wakefield and the simulated one still remains unknown. Since the discrepancy at all data points shows similar scale, it is likely due to a systematic error in the measurement. If this is the case, all measured data should be rescaled, and the transverse wakefield at the position of CLIC bunch separation (0.5 ns) is 5.5 V/(pC m mm), which still meets the beam dynamics requirement.

IV. CONCLUSIONS

The long-range transverse wakefield in CLIC accelerating structure was directly measured using beam-based techniques at the FACET facility. The conclusions are as follows.

(1) The long-range transverse wakefield of a 1.5 m length of CLIC prototype damped accelerating structure was directly measured with an unprecedented minimum resolution of 0.1 V/(pC m mm). The measured wakefield has been compared to computer simulations and good agreement found in the time structure of the wake for frequencies up to 50 GHz. The only discrepancy is an overall 10% amplitude disagreement. This level of precision validates the wakefield simulation techniques used in designing the CLIC main linac. It also gives a direct demonstration that the level of wakefield suppression, less than 6 V/(pC m mm) at the second bunch, 0.5 ns, necessary for beam stability can be achieved.

(2) The wakefield suppression of the CLIC structure design was shown to meet beam dynamics specifications: the measured wakefield at the position of CLIC bunch separation (0.5 ns) is less than 6 V/(pC m mm). This addressed an important feasibility issue for the future linear collider project.

ACKNOWLEDGMENTS

The authors thank Christine Clarke, Vitaly Yakimenko, and all operators in the FACET facility for their important

help during the measurement as well as Chris Adolphsen for sharing his experience with this kind of measurement. The authors also thank Paul Scherrer Institute (PSI) for financially supporting the structure construction through FORCE 2011 funding. This work performed under DOE Contract No. DE-AC02-76SF00515.

APPENDIX A: RESOLUTION OF MEASURED WAKEFIELDS

The resolution of the measured wakefield value was evaluated from the distribution of repeated measurements. As seen in Eq. (1) and Fig. 5, the final wakefield value was found computing the linear correlation between the electron beam deflection, k , and the transverse positron offset, Δy_p . This is expressed as below:

$$W_{\perp} = \frac{E_e}{Q_p L M} \sum_{m=1}^M \sum_{n=1}^N \frac{k(n, m) \Delta y_p(n)}{\Delta y_p^2(n)},$$

where n is the index of transverse positron offsets, m is the index of repeated data sets, and $k(n, m)$ is the deflection calculated from one measured electron trajectory. Other variables were introduced in Eq. (1). The equation can be rewritten as

$$W_{\perp} = \frac{1}{M} \sum_{m=1}^M \sum_{n=1}^N \lambda_n W_{\perp}(n, m),$$

where

$$\lambda_n = \frac{\Delta y_p^2(n)}{\sum_{i=1}^N \Delta y_p^2(i)},$$

and

$$W_{\perp}(n, m) = \frac{E_e}{Q_p L} \frac{k(n, m)}{\Delta y_p(n)}.$$

Each $W_{\perp}(n, m)$ is computed from a single measured trajectory, and W_{\perp} is the weighted average over all measurements, with λ_n as weights. The standard deviation is

$$\sigma(W_{\perp}) = \sqrt{\frac{1}{M} \sum_{m=1}^M \sum_{n=1}^N \lambda_n (W_{\perp}(n, m) - W_{\perp})^2}.$$

If one considers possible errors from the positron orbit bump, this standard deviation $W_{\perp}(n, m) - W_{\perp}$ must show a dependency on the positron offsets. This is denoted using the subscript n . In this case the standard deviation becomes

$$\sigma(W_{\perp})_2 = \sqrt{\frac{1}{M} \sum_{n=1}^N \lambda_n \left(\sum_{m=1}^M (W_{\perp}(n, m) - W_{\perp}) \right)^2}.$$

We defined as rms error of the wakefield measurement the maximum between the two standard deviations defined above, that is,

$$\text{MAX}(\sigma(W_{\perp 1}), \sigma(W_{\perp 2})) \sqrt{\frac{1}{M} \sum_{n=1}^N \lambda_n^2}$$

In this paper the resolution is defined as twice the rms error.

APPENDIX B: SETUP OF WAKEFIELD SIMULATION

We used the GDFIDL simulation code (version: 2015-01-21) [17] for the numerical wakefield estimation. The geometry used in the simulation was the same used as that of the structure built for the experiment, but implemented only 1 structure unit (whereas in the experiment six units were used). All metal surfaces in the geometry were assigned the perfect electrical boundary conditions. The diameter of beam pipes in both extremities were set to 8 mm, and the terminals of pipes were assigned PML (“perfect matched layer”) boundary conditions.

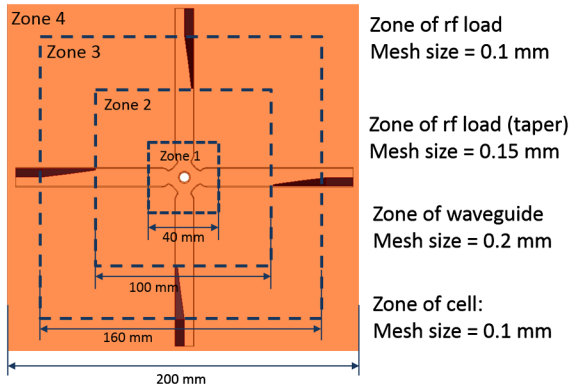


FIG. 12. Configurations of transverse mesh.

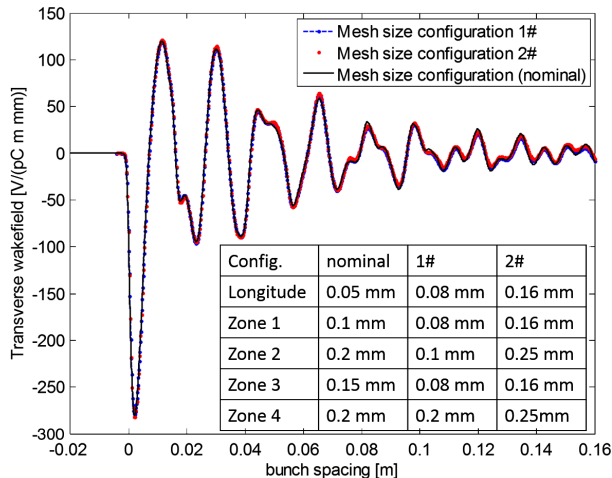


FIG. 13. Simulated results using different mesh size.

In the simulation the wakefields were excited by a positron bunch. The bunch traveled through the structure at the speed of light, with a trajectory parallel to the longitudinal axis with a 0.8 mm transverse offset. Another bunch was injected after the positron bunch to measure the wakefield voltage. The bunch distance was varied from 0 to 1 m using steps of 0.05 mm. Both bunches featured a Gaussian longitudinal charge density, with length σ_z 0.7 mm.

In the simulation, the longitudinal mesh size was 0.05 mm, compared to the length of a cell which is 8 mm. To use random-access memory (RAM) efficiently, we divided the geometry in four zones transversely, and adapted the mesh size (as seen in Fig. 12). We defined several GDFIDL fixed planes to have mesh planes exactly matching the metal surfaces of the geometry (wall of iris, waveguide, etc.).

Simulations using different mesh sizes were also carried out to check the dependency of the results on the mesh size. Figure 13 shows the result of three different mesh sizes: the first one is the nominal one, the second is a finer transverse mesh but coarser longitudinal mesh, and the last one features a coarser mesh both transversely and longitudinally. The discrepancy among them is about 1%–1.5% of the wakefield amplitude.

- [1] CLIC Conceptual Design Report (CDR), 2012, http://project-clic-cdr.web.cern.ch/project-CLIC-CDR/CDR_Volume_1.pdf.
- [2] D. Schulte, Multibunch calculations in the CLIC main linac, in *Proceedings of the 23rd Particle Accelerator Conference, Vancouver, Canada, 2009* (IEEE, Piscataway, NJ, 2009), FR5rfP055.
- [3] A. Grudiev and W. Wuensch, Design of the CLIC main linac accelerating structure for CLIC Conceptual Design Report, in *Proceedings of the 25th International Linear Accelerator Conference, LINAC-2010, Tsukuba, Japan* (KEK, Tsukuba, Japan, 2010).
- [4] T. Higo *et al.*, Comparison of high gradient performance in varying cavity geometries, in *Proceedings of the 4th International Particle Accelerator Conference, IPAC-2013, Shanghai, China, 2013* (JACoW, Shanghai, China, 2013), WEPFI018.
- [5] F. Tecker *et al.*, Experimental study of the effect of beam loading on rf breakdown rate in CLIC high-gradient accelerating structures, in *Proceedings of the 4th International Particle Accelerator Conference, IPAC-2013, Shanghai, China, 2013* (JACoW, Shanghai, China, 2013), THPEA013.
- [6] FACET facility in SLAC National Laboratory, http://portal.slac.stanford.edu/sites/ard_public/facet/Pages/default.aspx.
- [7] J. W. Wang *et al.*, Wakefield measurements of SLAC linac structures at the Argonne AATF, in *Particle Accelerator Conference, 1991. Accelerator Science and Technology., Conference Record of the 1991 IEEE* (IEEE, New York, 1991), Vol. 5, pp. 3219–3221.

- [8] C. Adolphsen, K. Bane, T. Higo, K. Kubo, R. Miller, R. Ruth, K. Thompson, and J. Wang, Measurement of Wake-Field Suppression in a Detuned X-Band Accelerator Structure, *Phys. Rev. Lett.* **74**, 2475 (1995).
- [9] T. Shintake *et al.*, The first wakefield test on the C-band choke-mode accelerating structure, in *Proceedings of the 18th Particle Accelerator Conference, New York, 1999* (IEEE, New York, 1999), FRA14.
- [10] I. Wilson *et al.*, An ASSET test of the CLIC accelerating structure, in *Proceedings of the European Particle Accelerator Conference, Vienna, 2000* (EPS, Geneva, 2000), THP2A18.
- [11] A. Latina, J. Pfingstner, D. Schulte, E. Adli, F. J. Decker, and N. Lipkowitz, Experimental demonstration of a global dispersion-free steering correction at the new linac test facility at SLAC, *Phys. Rev. ST Accel. Beams* **17**, 059901 (2014).
- [12] T. Weiland, N. Holtkamp, P. Schütt, R. Wanzenberg, W. Bialowons, M. Bieler, H.-C. Lewin, and F.-J. Decker, Status and future developments of the wakefield transformer experiment, *Nucl. Instrum. Methods Phys. Res., Sect. A* **298**, 93 (1990).
- [13] C. Jing *et al.*, Observation of wakefields in a beam-driven photonic band gap accelerating structure, *Phys. Rev. ST Accel. Beams* **12**, 121302 (2009).
- [14] R. A. Marsh, M. A. Shapiro, R. J. Temkin, E. I. Smirnova, and J. F. DeFord, Measurement of wakefields in a 17 GHz photonic band gap accelerator structure, *Nucl. Instrum. Methods Phys. Res., Sect. A* **618**, 16 (2010).
- [15] A. Latina *et al.*, Toolbox for applying beam-based alignment to linacs, in *Proceeding of the 27th Linear Accelerator Conference, LINAC-2014, Geneva, Switzerland* (JACoW, Geneva, Switzerland, 2014), THPP034.
- [16] H. Zha *et al.*, Beam-based measurements of long range transverse wakefields in CLIC main linac accelerating structure, in *Proceeding of 6th International Particle Accelerator Conference, IPAC-2015, Richmond, VA, USA* (JACoW, Richmond, 2015), TUPTY056.
- [17] W. Bruns, <http://www.gdfidl.com>.
- [18] C.-X. Wang, Model independent analysis of beam centroid dynamics in accelerators, Ph.D. dissertation, Stanford University, 1999.